5.3.2 **ARROW-2D**

For the fabrication of the second type of waveguides, the same technological steps as those of the rib ARROW (but with a different mask) can be used. However, in chapter 4 it was observed that ARROW-2D waveguides could be remotely coupled. Then, in order not to have uncontrolled directional couplers, devices based on ARROW-2D structures should be shielded. In this case, a two-mask process has been designed. Firstly, thick trenches will be defined on silicon. Inside each trench, a single device based on these waveguides will be placed. Then, any possible coupling between proximal structures will be avoided by the intermediate silicon wall, which would absorb any radiative modes.

Process starts with the growth of a thin silicon dioxide (0.2µm) on the silicon substrate, as shown in table 5.2. The first photolithographic step is followed by a dry silicon oxide etching that opens the windows on the SiO_2 where shielding trenches will be placed. After the silicon dry etching step (that defines the trenches), wafers are submerged in HF (49%) so as to remove the remaining silicon oxide mask.
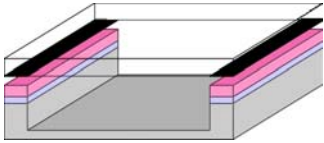
Shielding trenches for ARROW-2D waveguides		
	Silicon substrate. One-side polished, N-type, 4' diameter, 500µm thick	
	0.2µm wet thermal silicon dioxide	
	CNM-135 M1mask: Definition of the shielding trenches	
		Mask: Width: 200µm Length: 6000µm
		Step: 2 µm Positive photoresist SiO_2 RIE etching with CHF_3 Si RIE etching (3.8µm) with SF_6
	SiO_2 wet etching (HF 49%)	

Table 5.2: Fabrication steps for the shielding trenches of the ARROW-2D structure.

Once the micromechanized silicon has been achieved, the previously explained ARROW-A structure, with 2µm silicon dioxide, 0.35µm silicon nitride and 4.5µm silicon oxide are sequentially obtained, as shown in table 5.3. Si_3N_4 thickness has been varied as compared to previous ARROW-A configuration since the expected final height of the core is 3µm. After the second mask and a silicon oxide dry etching of

1.5μm, LAS are obtained. As it will be done with every integrated optical circuit, a 2μm-silicon oxide passivation is deposited on the entire wafer so as to protect the device from scratches or dust that could cause the waveguide not to work accordingly to specifications.
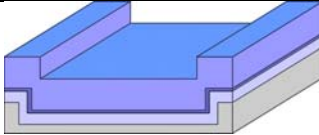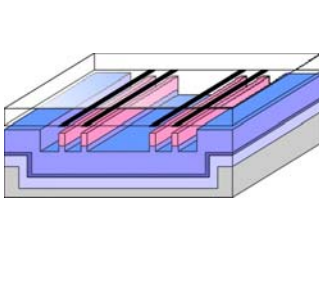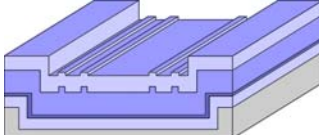
ARROW-2D waveguides		
	2nd cladding: 2μm wet thermal silicon dioxide. n=1.46	
	1st cladding: 0.38μm LPCVD silicon nitride. n=2.00	
	Core: 4.5μm PECVD silicon oxide. n=1.48	
	CNM-135 M2 mask: Definition of the ARROW-2D waveguides	
		Mask: Single and double lateral antiresonant structures LAS width: 3 μm. Waveguide width: 10,12,16,20 and 40μm. Waveguide expected final thickness: 3μm.
		Step: 2μm positive photoresist Definition of the antiresonant structures: 1.5μm SiO$_2$ RIE etching with CHF$_3$
	Passivation: 2μm PECVD silicon oxide. n=1.46 **Post process:** Cutting by a diamond blade Polishing with SIC (0.9μm)+ Al$_2$O$_3$ (0.3μm)	

Table 5.3: ARROW-2D final fabrication steps.

Analogously as it was done with the rib-ARROW waveguides, first measurements allowed obtaining the total losses as a function of the waveguide width. As can be seen in fig. 5.8, ARROW-2D waveguides behave exactly in the same way as rib-ARROW does, that is, total losses increase as the waveguide gets thinner. Again, this behavior can be associated to a minor light confinement of the mode on the waveguide as the core decreases. This assumption is confirmed when comparing the results obtained for waveguides with single and double LAS: it can be seen that for a given waveguide width, losses are much lower in the latter case. Moreover, the width value at which losses sharply increase is also much lower for waveguides with double LAS.
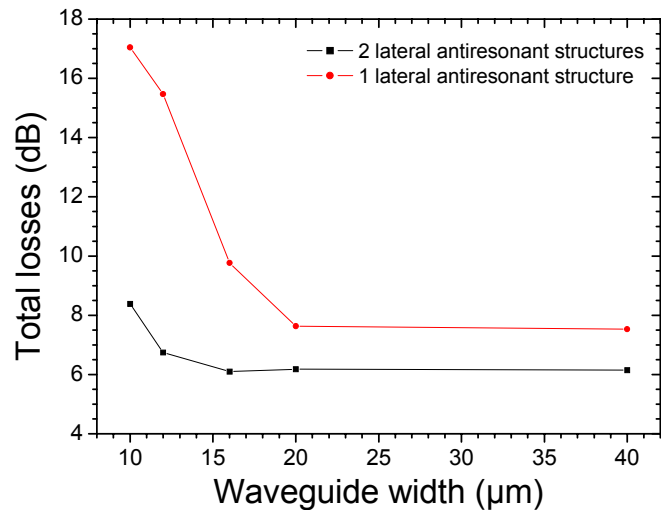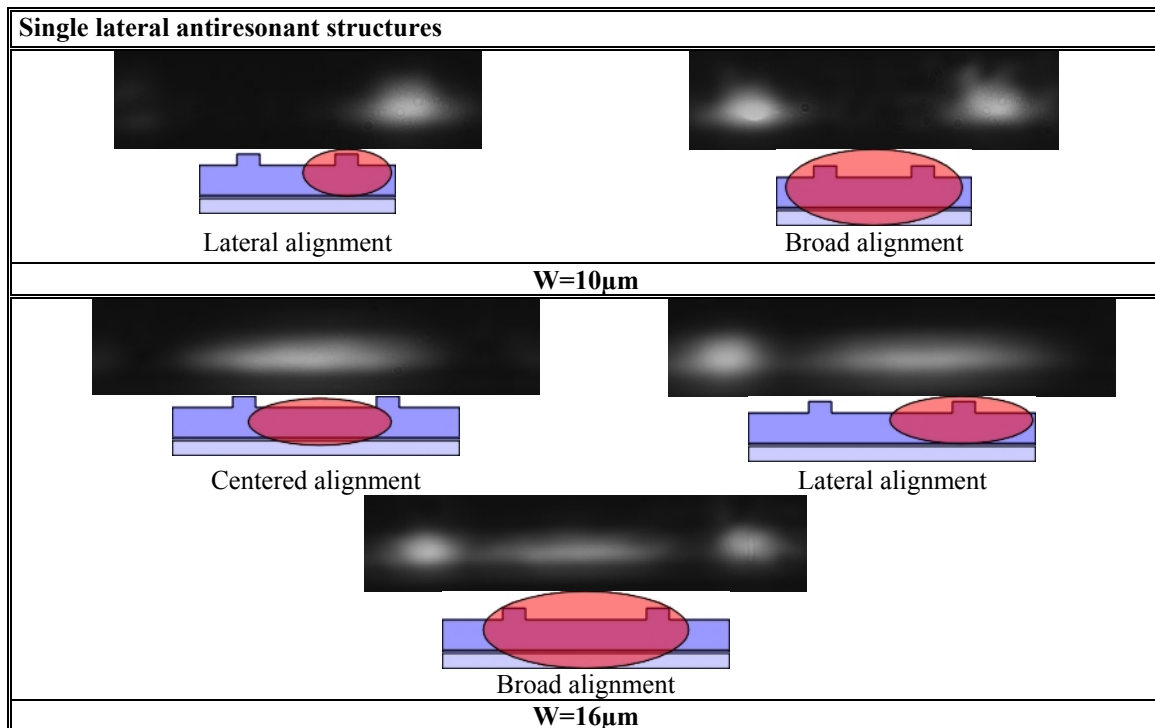
Fig 5.8: Total losses as a function of the core width for ARROW-2D waveguides with one or two lateral antiresonant structures.

Finally, it can be seen that, as it also happened with rib ARROW waveguides, losses seem to be independent of the waveguide width above a certain size, being its value 7.53dB and 6.14dB for single and double lateral antiresonant structures, respectively. The fact that only five waveguides with different widths have been obtained does not allow to confirm this latter assumption, but at least, a clear tendency to a stable losses value as core widens is observed. Moreover, only one length of 6000µm was available at the CNM-135 masks, thence, insertion losses could not be obtained. However, it is expectable that its value would be similar than the rib-ARROW structures.

Different near field images were taken of ARROW-2D waveguides with single and double LAS. Firstly, single-mode fiber optics was aligned at the center of the waveguide and the output intensity profile was obtained. Then, input fiber was progressively misaligned so as to determine whether was possible to excite any higher order mode apart from these of the LAS. Finally, fiber was placed again at the center of the waveguide, but this time a larger distance was left between the fiber optics and the waveguide. Thus, input field was broad enough so as to couple simultaneously light into the LAS and into the waveguide. That allowed obtaining information concerning the relative intensity between the modes of the whole structure.

The near field profiles of ARROW-2D waveguides with single LAS are shown in fig. 5.9. As can be seen, for core width below 16μm, power is coupled at the lateral antiresonant structures and no excitation of the expected ARROW-2D fundamental mode is observed. When waveguides are 16μm width, TE_{00} mode can be excited when light is coupled into the waveguide. As the fiber optics is progressively misaligned, it can be observed that fundamental mode decreases in amplitude but its shape does not vary, meaning that these waveguides are single-mode. If light is injected in the whole structure, it can be observed that the amount of light coupled on the LAS is higher as compared to these in the waveguide. However, for a width of 20μm, single-mode behavior is still observed and with broad excitation light is equally coupled on the LAS and on the waveguide. Finally, for waveguides with a core width of 40μm, as input fiber was progressively misaligned, three different modes were observed. Although this result is in agreement with the simulations done in chapter 4, the non-uniform field distribution in the waveguide could lead to the conclusion that there may be fabrication defects or impurities in this device. Thence real modal properties of this last waveguide could be different as these observed in the near field image shown in fig.5.9.
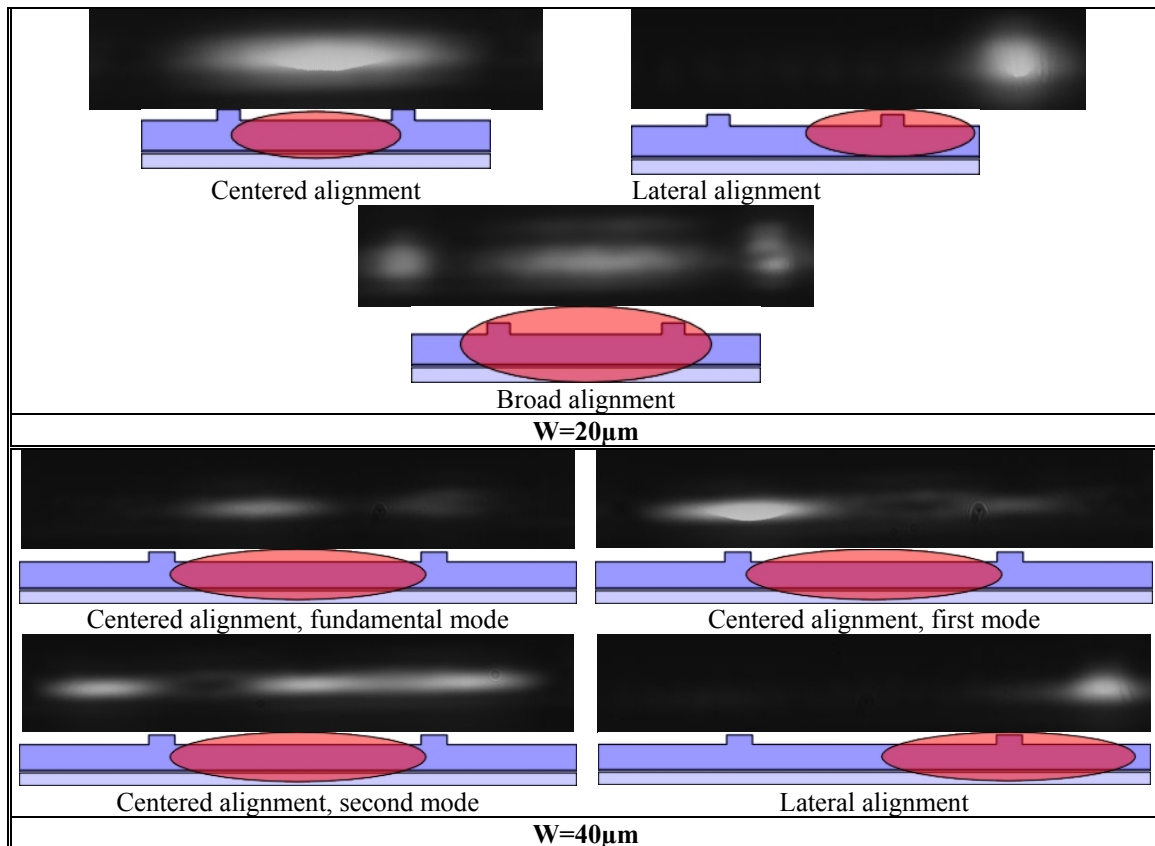

Single lateral antiresonant structures

Lateral alignment — Broad alignment

W=10μm

Centered alignment — Lateral alignment

Broad alignment

W=16μm

Fig 5.9: Near field images of the ARROW-2D waveguides with single lateral antiresonant structures.

It was shown in chapter 4 that a double lateral antiresonant structure should provide with higher confinement as compared to the previously measured configuration. Near field results of this structure are shown in fig. 5.10. As can be seen, 10-μm width waveguides are able to support the TE_{00} mode, as opposite to the single lateral antiresonant structures with the same width. Using broad injection, it can be observed that power coupled in the waveguide of 20μm is higher that these propagating in the lateral antiresonant structures while keeping its single-mode properties unaltered. Finally, for the widest waveguides, only two different modes can be observed in the waveguide. The shape and distribution of the lobes in the waveguide is now clearer than the case of single lateral antiresonant pairs, confirming the existence of only two modes in a 40μm-width, 3μm-height waveguide.